
Supporting Information

Enhancing photo-driven seawater splitting performance of hierarchical TiO₂ through rich surface hydroxyls and oxygen vacancies design

Ya-Jiao Zhang, Shi-Tian Xiao, Yi-Tian Wang, Feng-Juan Wu, Si-Ming Wu, Lu Wu, Fu-Fei Pu, Li-Ying Wang, Ge Tian, Cong-Yun Huang and Xiao-Yu Yang**

1. Experimental Procedures

1.1 Chemicals

Commercial 40 nm anatase TiO₂ nanoparticles (designed as Comm-TiO₂, AR) was purchased from Aladdin. NaOH (AR), NaCl (AR), Na₂SO₄ (AR), hydrochloric acid (36 wt. %, AR) and methanol (AR) were provided by Sinopharm Chemical Reagent Co. Deionized water was used in all experiments.

1.2 Synthesis of TiO₂ nanofibers

In a typical synthesis, 10.5 g NaOH and 0.5 g Commercial 40 nm anatase TiO₂ nanoparticles was stirred in 30 ml of deionized water to achieve uniform dispersions of TiO₂ in NaOH solution. Then the mixture was transferred to a Teflon-lined autoclave. The mixture was heated at 120 °C for 24 h. After the autoclave was cooled to room temperature naturally, the obtained product was filtered and stirred overnight in 0.1M HCl solution. The product was washed with deionized water for several times, filtered, dried at 80 °C. Then the resulting TiO₂ (As-TNF) nanofibers were calcined at 300 °C, 400 °C, 500 °C, 600 °C, 700 °C for 1 h (designed as TNF-300, TNF-400, TNF-500, TNF-600, and TNF-700, respectively), and the heating rate to the target temperature is 1 °C/min.

2. Characterization

Thermogravimetric analysis (TGA) was conducted using a NETZSCH STA 449 F3 thermogravimetric analyzer with a heating rate of 5 °C min⁻¹ under air. Scanning electron microscopy (SEM) images were taken with an S-4800 electron microscope operating at 5 kV to observe the morphology. Powder X-ray diffraction (XRD) patterns were recorded by a D8 Advance X-ray diffractometer (Bruker, Germany) with Cu-K α radiation ($\lambda = 0.15406$ nm) operated at 40 kV, 40 mA. The nitrogen adsorption and desorption isotherms of As-TNF, TNF-300, TNF-400, TNF-500, TNF-600, and TNF-700 were measured using a Micromeritics ASAP 2020M system. Before the measurements, the samples were outgassed at 120 °C in vacuum for 12 h. The BET surface area was determined by a multipoint BET method using the adsorption data in a relative pressure (P/P₀) range of 0.05–0.3. The Barrett–Joyner–Halenda (BJH) method was used to determine the pore sizes. Electron paramagnetic resonance (EPR) measurements were performed at the X-band using a JEOL FA 2000 spectrometer. The microwave frequency was 9.131 GHz, the modulation amplitude was 0.1 mT, the microwave power was 1 mW, and the experimental temperature was 295 K. X-ray photoelectron spectra (XPS) of the samples were recorded on a PHI Quantera II, (ULVAC-PHI, Japan) using a monochromated Al-K α X-ray source. Accurate binding energies (± 0.1 eV) were determined with respect to the position of the adventitious C 1s peak at 284.8 eV. X-ray photoelectron spectra (XPS) of the samples were recorded on a PHI Quantera II, (ULVAC-PHI, Japan) using a monochromated Al-K α X-ray source. Accurate binding energies (± 0.1 eV) were determined with respect to the position of the adventitious C 1s peak at 284.8 eV. Fourier-transform infrared (FT-IR) spectra were obtained with a Nicolet Avatar 360 spectrometer. Ultraviolet–visible spectroscopy diffuse

reflectance spectra (UV–vis DRS) were attained using a Shimadzu UV–vis spectrophotometer (UV-2550). ^1H MAS and 2D ^1H DQ-SQ spectra were recorded in a 1.9 mm MAS probe on a Bruker AVANCE-III 500 spectrometer with a sample spinning rate of 30 kHz, a 1H $\pi/2$ pulse length of 1.65 μs and a recycle delay of 5 s.

3. Photocatalytic Experiment.

Photocatalytic H_2 production was performed in a closed circulation system using a PLS-SXE-300D lamp (Beijing Perfectlight Technology Co., Ltd.) with UV-vis light. The lamp was 10 cm away from the reaction solution. 20 mg of sample was suspended in 80 mL of an aqueous solution containing 40 mL H_2O (or simulated seawater (3.5wt.%NaCl) or natural seawater (Zhuhai Sea)), 40 mL methanol and 5.2 μL H_2PtCl_6 (100 mmol/L). The mixture was sealed in a quartz vessel and vacuumed for 15 min to remove the dissolved oxygen, a continuous magnetic stirrer and circulating cooling water was applied during the experiment, and temperature in the quartz reaction vessel is about 25°C . The produced H_2 was analyzed by an Agilent 7890 A gas chromatograph (GC) with a thermal conductivity detector (TCD).

4. Photoelectrochemical Measurements.

The photoelectrochemical measurements were carried out on an electrochemical workstation (Autolab PGSTAT302N), including the photocurrent tests and electrochemical impedance spectra (EIS), linear sweep voltammograms (LSV), OCP and Tafel curves. Photocurrent tests were carried out in a conventional three-electrode with a Pt foil as the counter electrode and a saturated silver chloride electrode the reference electrode under a PLS-SXE-300C lamp. The working electrodes were prepared by dispersing catalysts (5 mg) and Nafion solution (10 μL , 5 wt%) in water/ethanol mixed solvent (500 μL , 1:1 v/v) at least 10 min of sonication to form a

homogeneous ink. Then the working electrodes were synthesized by drop-casting the above ink (25 μL) onto FTO glass with an area of 1 cm^2 . When testing the photocurrent, the distance between the lamp and the working electrode was 10 cm. After 600 s of illumination, the photocurrent remained stable. At this point, shading and illumination began alternately, shading and illumination duration were both 50 s, with a total of 5 testing cycles. EIS were obtained with a frequency range of 100 kHz to 0.01 Hz. The electrolyte used to test photocurrent and EIS is 0.5 M Na_2SO_4 solution. The linear sweep voltammograms (LSV) were operated at 10 mV s^{-1} in a potential range from -0.7 to 0.7 V vs Ag/AgCl both in dark and under illumination. The electrolyte used to test LSV was 0.1M PBS solution (0.1 M KH_2PO_4 , 0.1 M Na_2HPO_4 , 0.6 M NaCl). In order to prevent the sample from falling off the FTO glass during the test, the working electrodes above were calcined at 300 $^\circ\text{C}$ for two hours. The experimental setup of OCP and Tafel curves consisted of two coupled cells, a corrosion cell and a photoelectrochemical cell. The electrolyte in the corrosion cell was 3.5 wt% NaCl, while the photoelectrochemical cell electrolyte was 0.1 M Na_2S and 0.2 M NaOH. An ion exchange membrane was used to connect the two electrolyte solutions. The photoelectrochemical cell is a conventional three-electrode system. Na_2S functioned as the scavenger and inhibited S^{2-} hydrolysis by the addition of NaOH. The 304SS electrode in the corrosion cell connected to working electrode in the photoelectrochemical cell, working electrode is the same as in the photocurrent tests. Pt sheet and Ag/AgCl as counter and reference electrodes, respectively. The Tafel curves were measured in the range of -0.8V to 0.2 V versus OCP.

5. Density Functional Theory Calculations.

All models were built using Materials Visualizer interface of BIOVIA Materials Studio 2017

(17.1), and structural optimization and energy calculations were performed using the Dmol3 module under BIOVIA Material Studio 2017 software. The generalized gradient approximation of Perdew–Burke–Ernzerh was used as the exchange correlation functional in the Kohn-Sham equation, and the all-electron double numerical basis set with polarization function (DNP 4.4version) was used for all atoms. The DFT-D Grimme method was used to correct the long-range interaction of carbon atoms in the system. The surface structure was obtained by the optimized protocell. The thickness of (101) surfaces of anatase including the vacuum layer is 24.49 Å with total of 6 layers containing 24 Ti atoms and 48 oxygen atoms. Then, the surface model of hydroxyl TiO₂ were constructed on the basis of the optimized TiO₂ surface. The convergence standard of structural optimization was set as: a) 2×10^{-5} Hartree energy tolerance; b) 1×10^{-5} Hartree SCF tolerance; c) 5×10^{-3} Å maximum displacement tolerance; and d) 4×10^{-3} Hartree/Å maximum force tolerance. The convergence standard of and energy calculation was set as: a) 1×10^{-5} Hartree SCF tolerance. After the system fully relaxes, adsorption energy (E_{ad}) was used to evaluate the stability of H or heteroatoms adsorbed on surface, which is defined as:

$$E_{ad} = E_{Total} - E^* - E_n$$

E_{Total} is the energy of the whole system; E* represents the energy of surface system; E_n represents the energy of adsorbed H or heteroatom.

Supplementary tables:

Table S1. BET surface, pore volume and pore diameter of As-TNF, TNF-300, TNF-400, TNF-500, TNF-600 and TNF-700.

Samples	S_{bet} (m^2/g)	Pore volume($\text{cm}^3 \text{g}^{-1}$)	Pore diameter (nm)
As-TNF	327	0.75	11
TNF-300	257	0.69	11
TNF-400	177	0.59	12
TNF-500	113	0.52	17
TNF-600	67	0.38	19
TNF-700	26	0.19	28

Table S2. Summary of the TiO₂-based materials in photocatalytic water, simulated and natural seawater splitting.

Photocatalyst	Light source	H ₂ production rate (mmol h ⁻¹ g ⁻¹)	t>9 0% (h)	System	Ref.
1wt% Pt/TiO ₂	300 W Xe lamp	52	21	Natural seawater	Our work
1wt% Pt/TiO ₂	300 W Xe lamp	79		Simulated seawater	Our work
Pt/TiO ₂	500 W Hg lamp	0.555	-----	Natural seawater	(Nano Res. 2022) ^[1]
0.5wt% Pt/TiO ₂	300 W Xe lamp	25.9	15	Simulated seawater	(Chem. Eur. J 2021) ^[2]
Co ₃ O ₄ @C/TiO ₂	UV-LED lamp (25 W, 365 nm)	11.4	20	water	(J. Environ. Chem. Eng. 2021) ^[3]
Cu ₂ O/TiO ₂	300 W Xe lamp	5.1	24	Natural seawater	(J. Alloys Compd 2021) ^[4]
Pt-brookite TiO ₂	UV light	0.0072	10	Natural sea water	(Nano Energy 2020) ^[5]
Mo _x S@TiO ₂ @Ti ₃ C ₂	300 W Xe lamp (AM-1.5)	10.51	-----	Water	(Chem. Eng. J 2020) ^[6]
5% CuO/TiO ₂	300W Xe lamp	2	15	water	(J. Alloys Compd 2020) ^[7]

Supplementary figures:

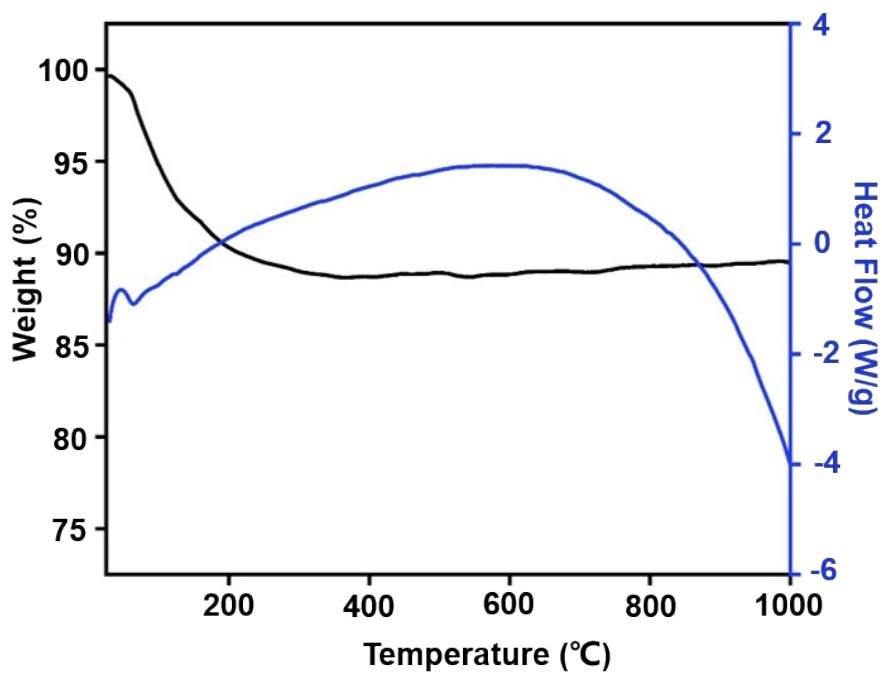


Figure S1. Thermogravimetric curves of As-TNF.

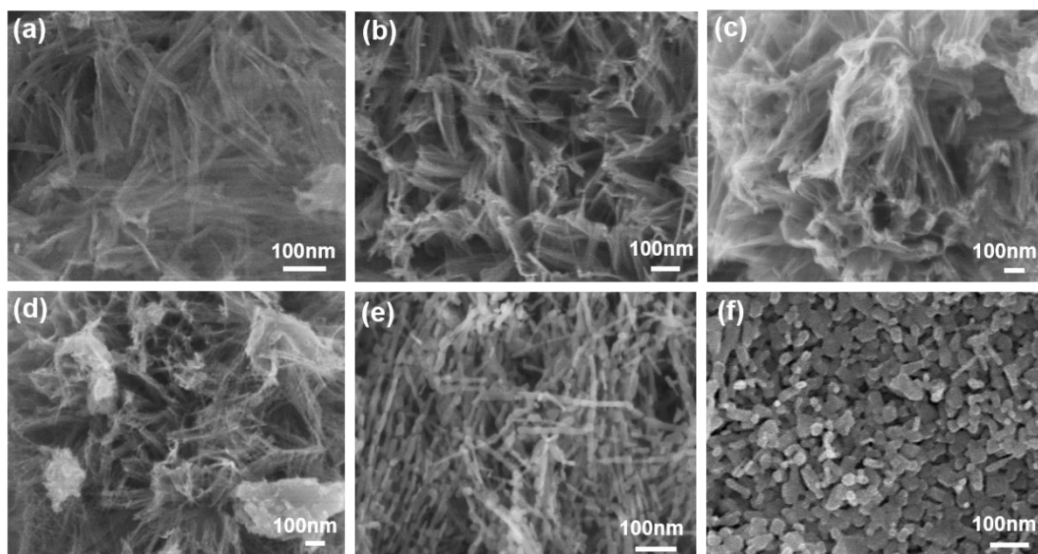


Figure S2. SEM images of (a) As-TNF, (b) TNF-300, (c) TNF-400, (d) TNF-500, (e) TNF-600 and TNF-700.

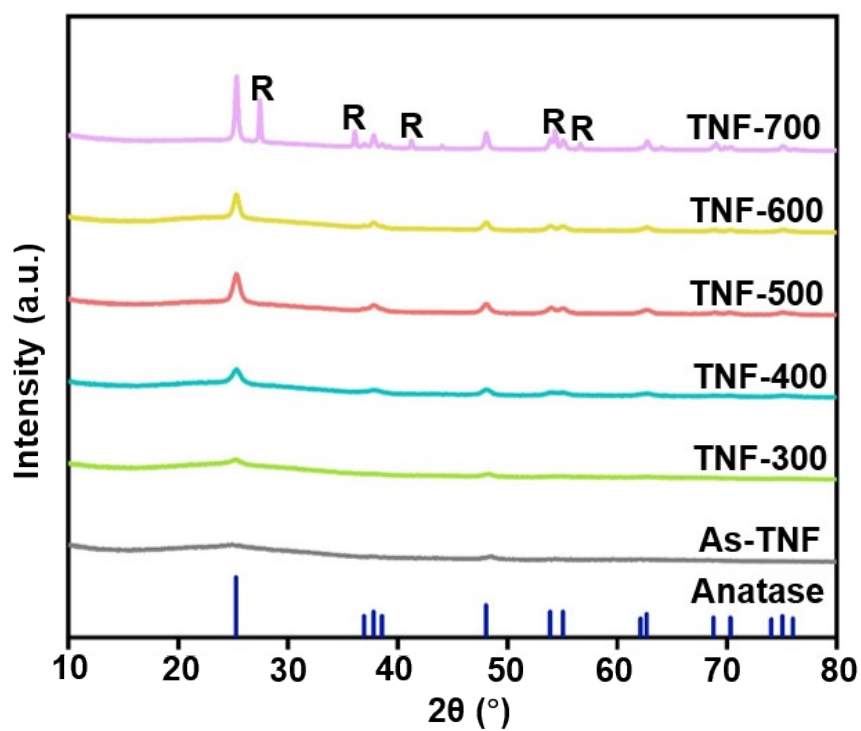


Figure S3. XRD patterns of As-TNF, TNF-300, TNF-400, TNF-500, TNF-600 and TNF-700.

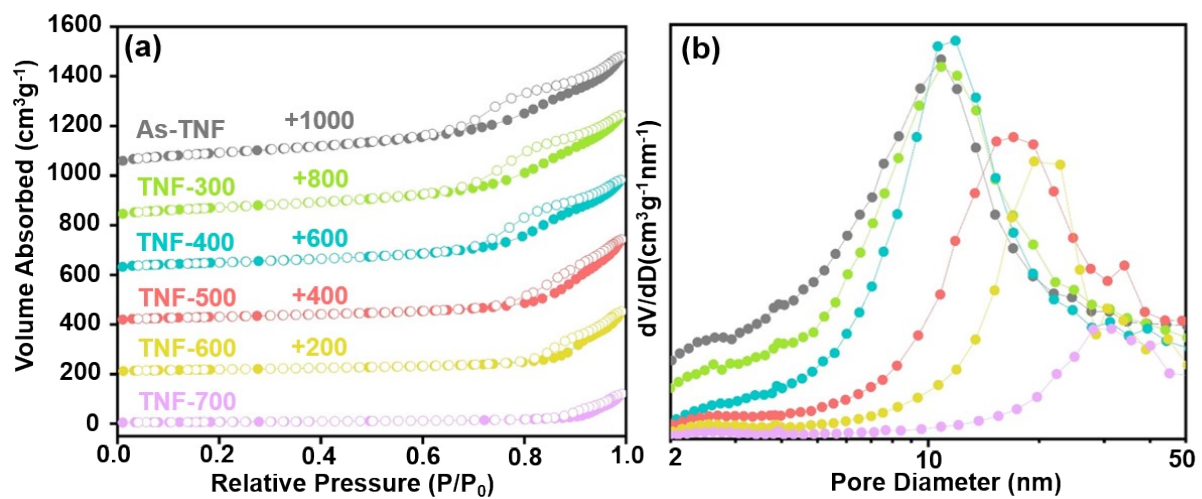


Figure S4. (a) Nitrogen-adsorption–desorption isotherms and (b) corresponding pore size distribution of As-TNF, TNF-300, TNF-400, TNF-500, TNF-600 and TNF-700.

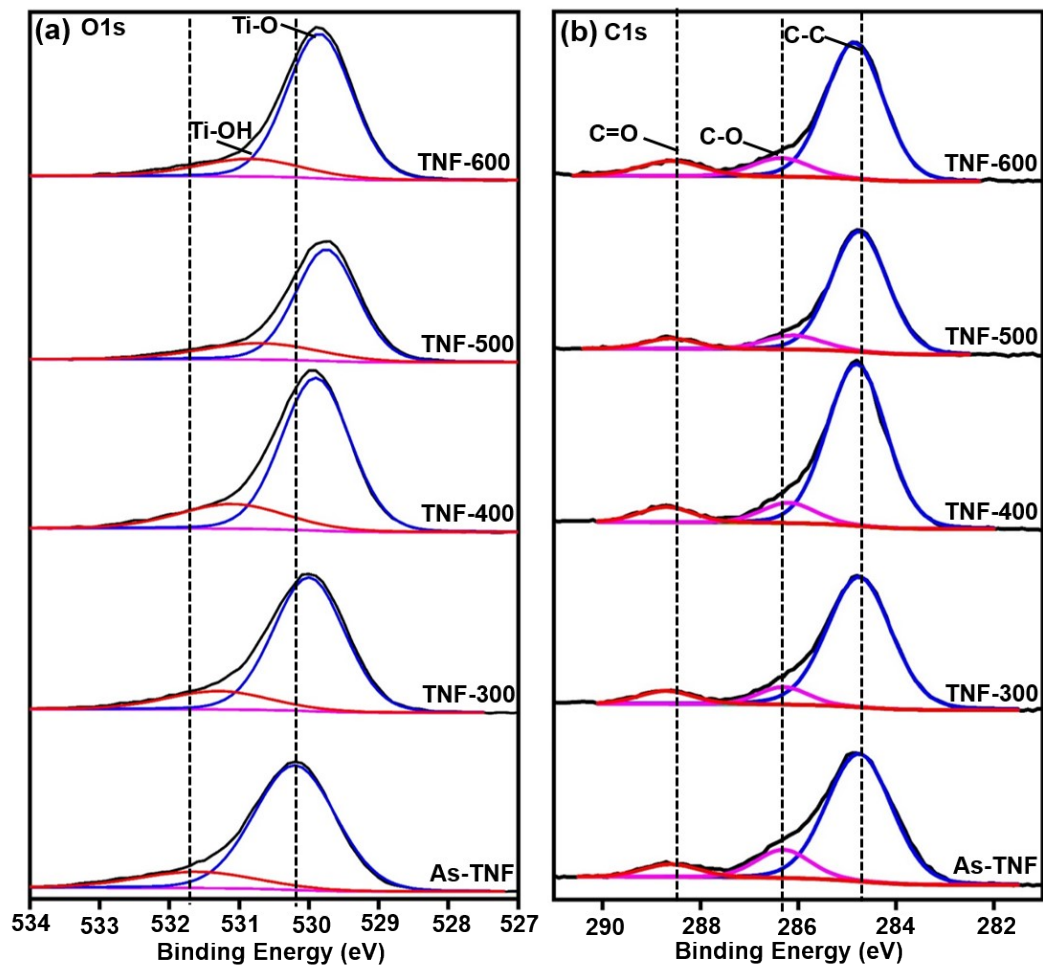


Figure S5. (a) O 1s XPS spectra of As-TNF, TNF-300, TNF-400, TNF-500 and TNF-600. (b) C 1s XPS spectra of As-TNF, TNF-300, TNF-400, TNF-500 and TNF-600.

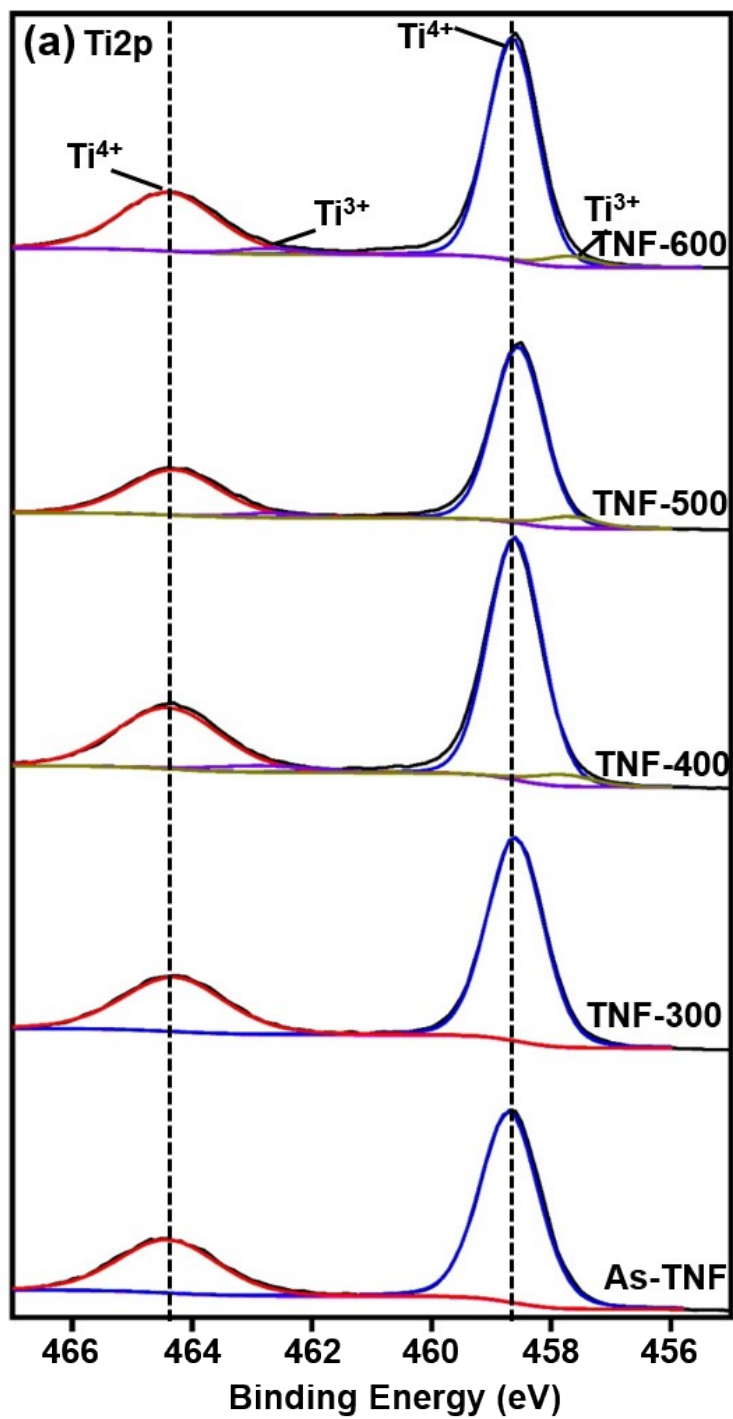


Figure S6. (a) Ti 2p XPS spectra of As-TNF, TNF-300, TNF-400, TNF-500 and TNF-600.

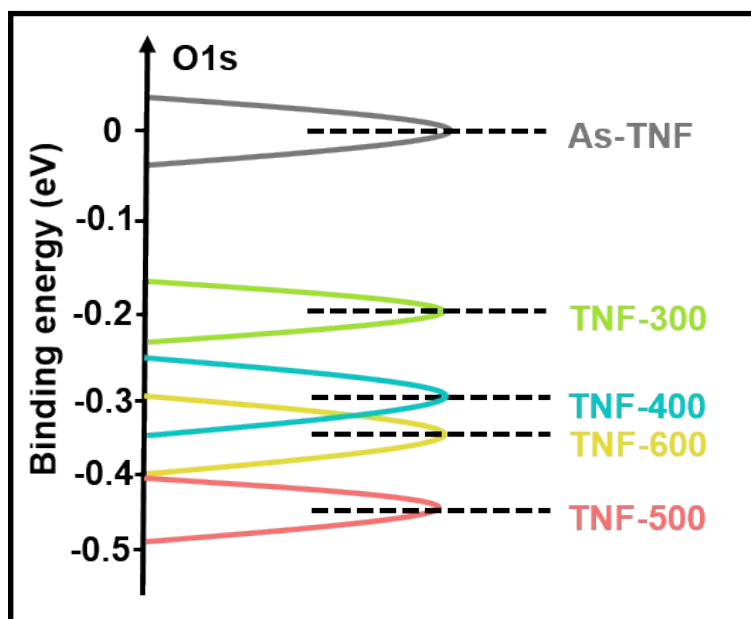


Figure S7. O1s chemical shift among As-TNF, TNF-300, TNF-400, TNF-500 and TNF-600

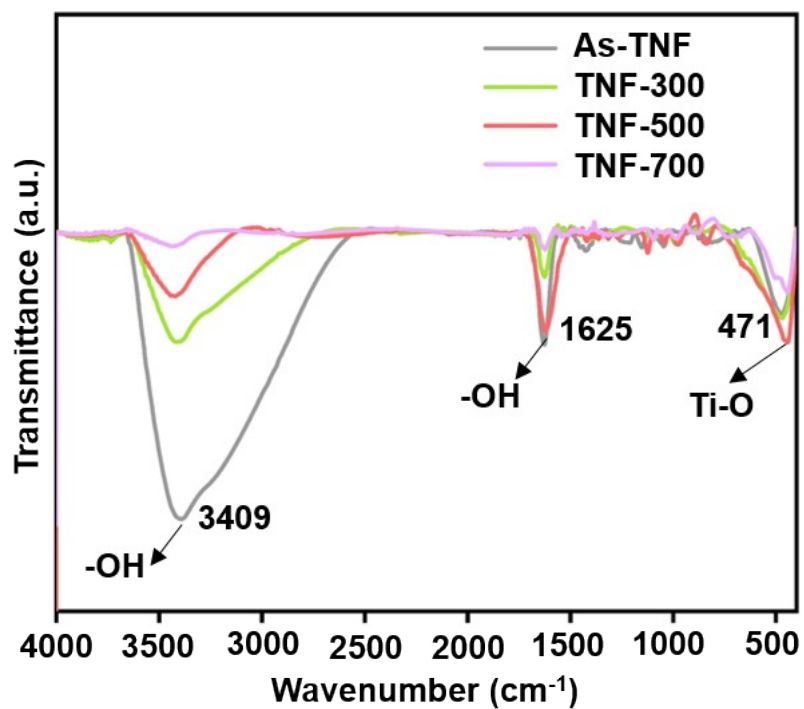


Figure S8. FT-IR spectra of As-TNF, TNF-300, TNF-500 and TNF-700.

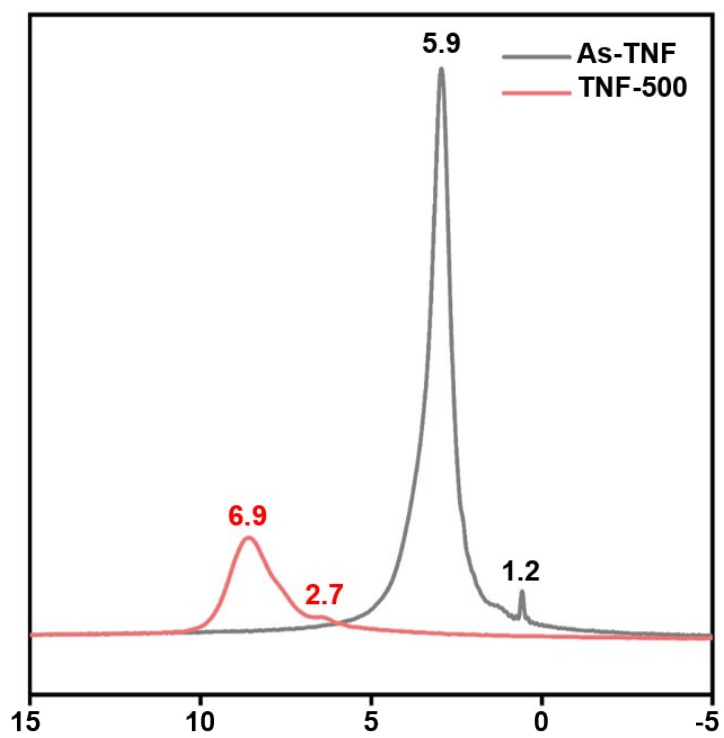


Figure S9. Solid-state ^1H MAS NMR spectrum of As-TNF and TNF-500.

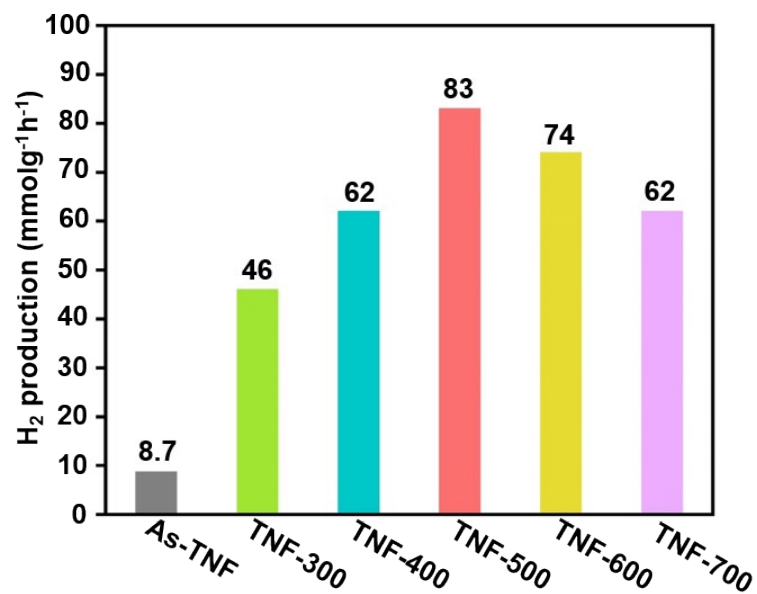


Figure S10. photocatalytic activity for the H₂ production of As-TNF, TNF-300, TNF-400, TNF-500, TNF-600 and TNF-700 in water.

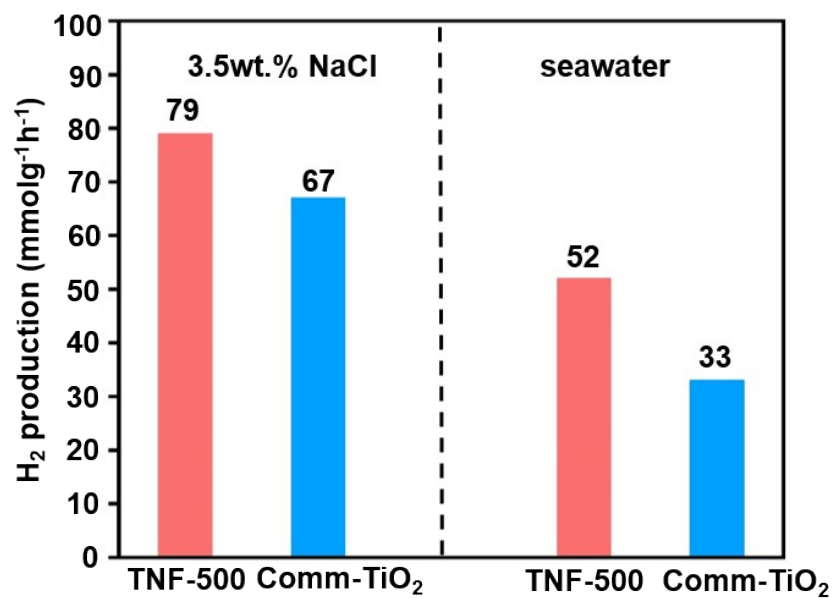


Figure S11. Photocatalytic activity for the H₂ production of TNF-500 and commercial 40 nm TiO₂ in 3.5 wt. % NaCl solution and seawater.

The material used in the synthesis of nanofibers is commercial anatase titanium dioxide with a particle size of 40 nm, so the photocatalytic hydrogen production rates of TNF-500 and 40 nm commercial TiO₂ are compared here.

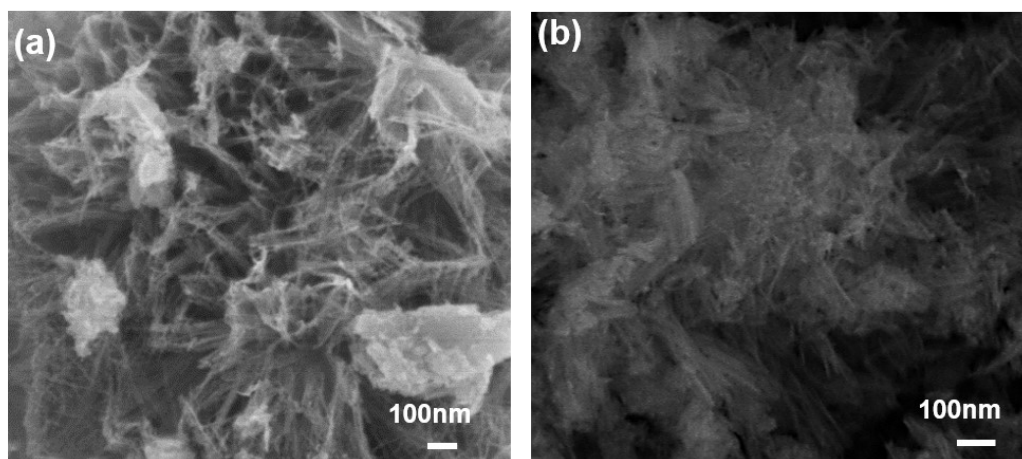


Figure S12. SEM images of TNF-500 (a) before and (b) after 21 h-photocatalytic stability measurement.

After 21 hours of stability measurement of photocatalytic hydrogen production in seawater, the surface of TNF-500 was still distributed with nanofibres and the surface morphology did not change significantly.

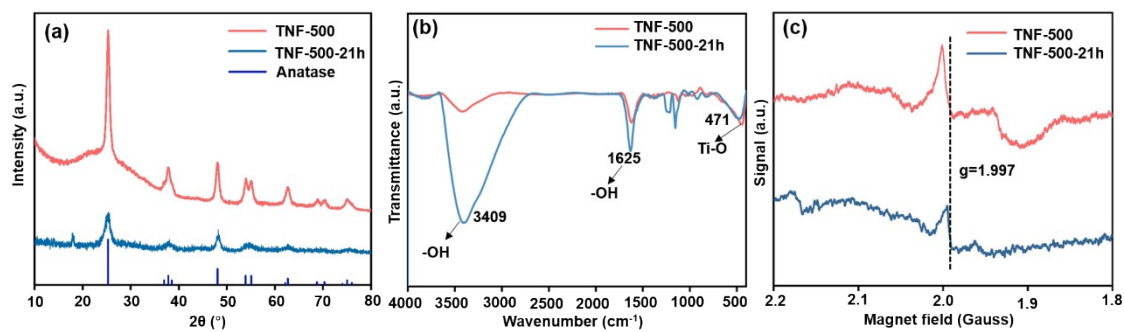


Figure S13. (a)XRD spectra, (b) FT-IR spectra and (c) EPR spectra of TNF-500 before and after 21 h-photocatalytic stability measurement.

XRD, FTIR and EPR measurements revealed that the crystallinity of TNF-500 was reduced after stability testing, but surface hydroxyl groups and oxygen vacancies were still existing.

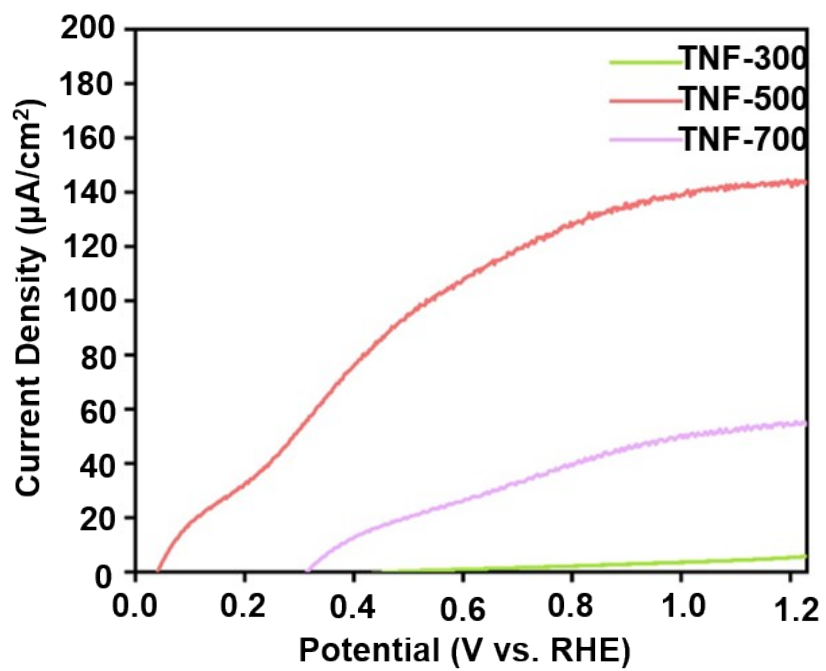


Figure S14. LSV curves of TNF-300, TNF-500 and TNF-700.

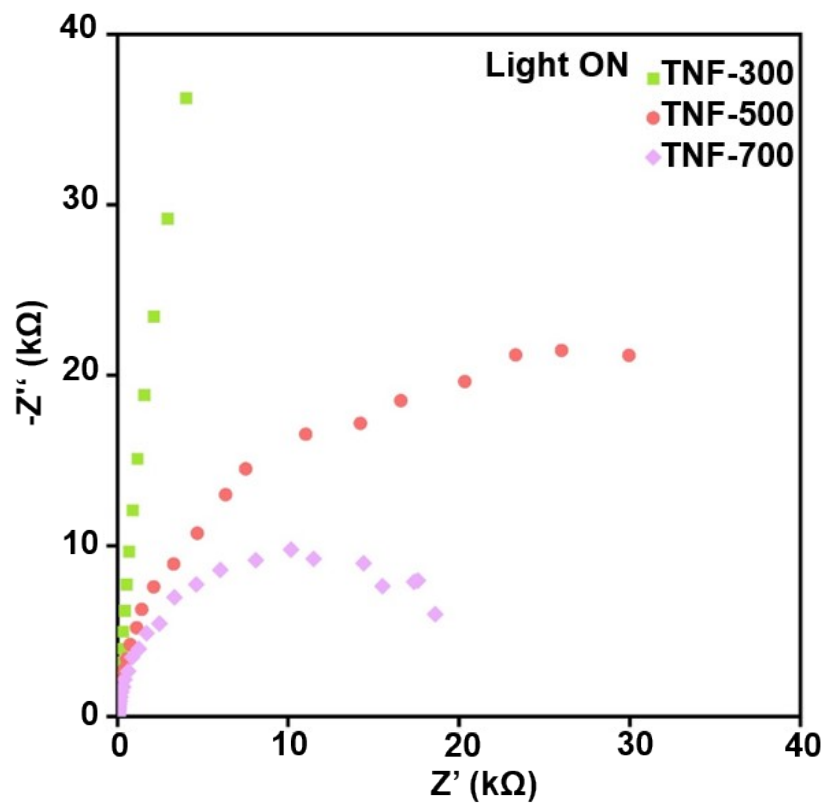


Figure S15. EIS Nyquist plots of TNF-300, TNF-500 and TNF-700.

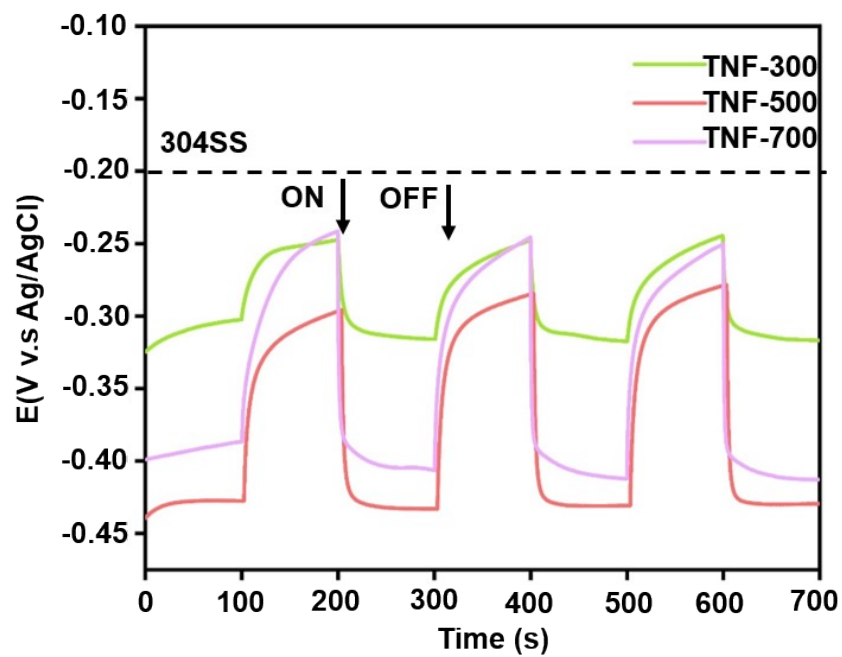


Figure S16. The open circuit voltage of TNF-300, TNF-500, TNF-700.

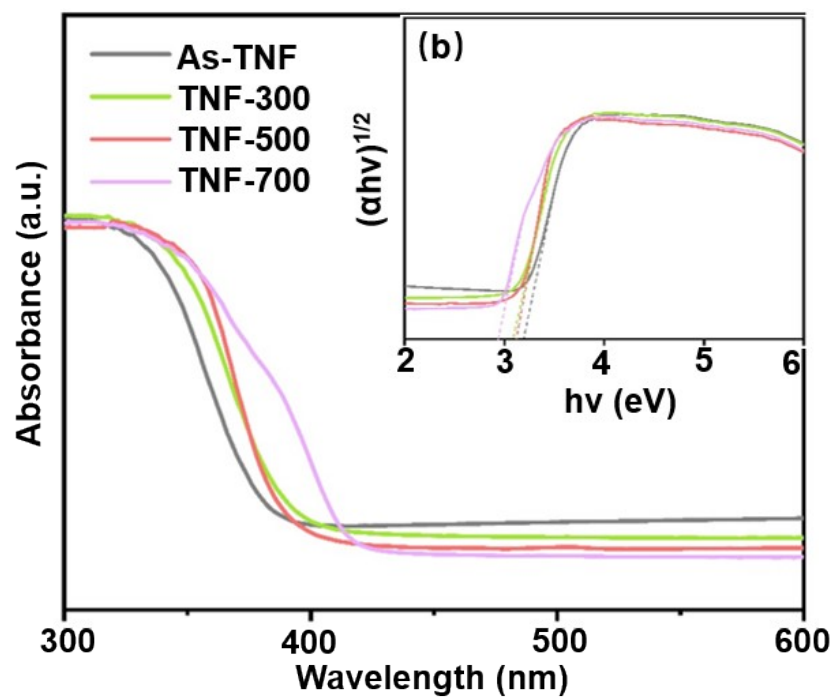


Figure S17. UV-vis diffuse reflectance spectrum of As-TNF, TNF-300, TNF-500 and TNF-700. The inset in (b) Curves of Kubelka-Munk function as the vertical axis and plotted against the photon energy.

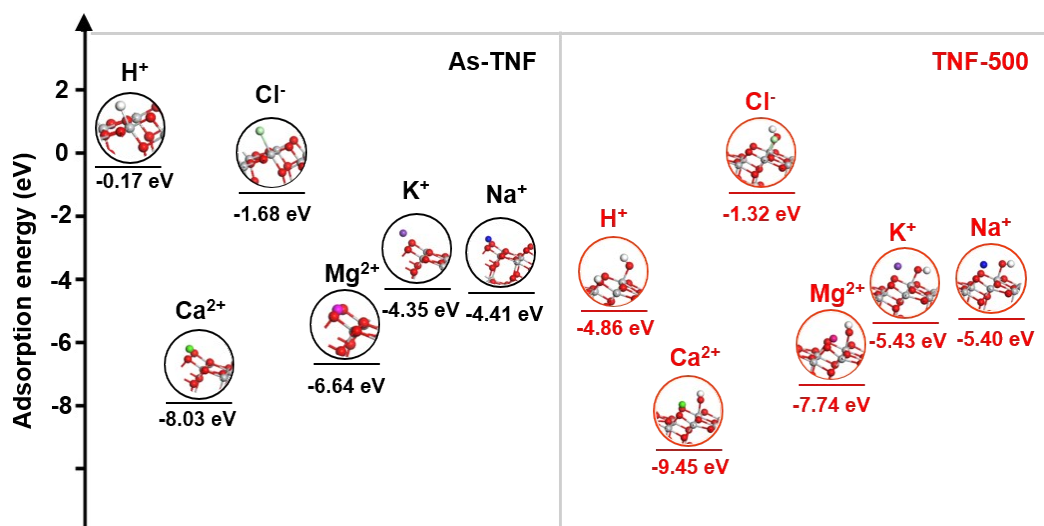



Figure S18. DFT calculated (DMol3 program) structures and adsorption energies of ions in seawater with As-TNF and TNF-500.

-
- 
- [1] J.N. Zhang, Y.F. Lei, S.A. Cao, W.P.Hu, L.Y. Piao, X.B. Chen, *Nano Res.*, 2022, **15**, 2013.
- [2] Y. X. Zhang, S. M. Wu, G. Tian, X. F. Zhao, L. Y. Wang, Y. X. Yin, L. Wu, Q. N. Li, Y. X. Zhang, J. S. Wu, C. Janiak, K. I. Ozoemena, M. Shalom, X. Y. Yang, *Chem. Eur. J.* 2021, **27**, 14202.
- [3] H. M. El-Bery, H. N. Abdelhamid, *J. Environ. Chem. Eng.* 2021, **9**, 105702.
- [4] S. Lv, Y. Wang, Y. Zhou, Q. Liu, C. Song, D. Wang, *J. Alloys Compd.* 2021, **868**, 159144.
- [5] S. Cao, T.-S. Chan, Y.-R. Lu, X. Shi, B. Fu, Z. Wu, H. Li, K. Liu, S. Alzuabi, P. Cheng, M. Liu, T. Li, X. Chen, L. Piao, *Nano Energy* 2020, **67**, 104287.
- [6] Y. Li, L. Ding, Z. Liang, Y. Xue, H. Cui, J. Tian, *Chem. Eng. J.* 2020, **383**, 123178.
- [7] Y. Wang, M. Zhou, Y. He, Z. Zhou, Z. Sun, *J. Alloys Compd.* 2020, **813**, 152184.